International Journal of Scientific Engineering and Research (IJSER)
ISSN (Online): 2347-3878
Index Copernicus Value (2015): 62.86 | Impact Factor (2015): 3.791

Encapsulation viz Capping: Controlled Growth of ZnO Nanophosphor

Prinsa Verma*, Avinash C. Pandey[1]

Nanophosphor Application Center[1], Allahabad University, India
Department of Space, New Delhi*, India

Abstract: ***We reported effective encapsulation and capping of ZnO nanoparticles by using Organic and Inorganic stabilizers. And studied the phenomenon that the intensity of the ultraviolet (UV) photoluminescence (PL) from ZnO was greatly enhanced by incorporating ZnO into the SiO2 matrix as compared to Poly Vinyl Pyrollidone (PVP) capping. PL excitation results show that both the ZnO nanoparticles and the SiO2 matrix in the nanocomposites contribute to the luminescence process for the UV band. ZnO–SiO2 nanocomposite consisting of ZnO nanoparticles embedded in a SiO2 matrix and ZnO capped with Poly Vinyl Pyrollidone both were prepared by the sol–gel technique. Annealing in the range 100-700 degC in air atmospheres showed high stability of the particle radius due to effective encapsulation within the silica matrix as compared to PVP Capping. Temperature dependent studies shows inorganic encapsulation seemed to be the better than organic capping as it can withstand high temperature, also having much higher luminescence intensity and shows monodispersity of the ZnO nanoparticles. The size of the nanocrystals and nature of their capping, directly influences - Thermal stability, Optical properties, mechanical support and monodispersity which are important parameters for device fabrication. Encapsulation is carried out for increasing persistence time and controlled release of nanoparticles in different environmental conditions.***

Keywords: Encapsulation, Nanocomposites, Photoluminescence

1. Introduction

Zinc oxide (ZnO) is a wide band gap (3.37 eV) semiconductor with a large exciton binding energy, (60 meV) [1], in which the exciton governed luminescence at short wavelengths is leading at room temperature. ZnO can be either zinc blende or wurtzite structure [2], mostly ZnO found to be crystallize in the hexagonal wurtzite structure [3, 4]. The discovery of ultraviolet (UV) lasing effects [4, 5] from ZnO has promoted great interest in the study of its luminescence properties. ZnO can emit three luminescence bands in the UV, green, and yellow spectral range [6]. The UV (~3.3eV) emission is mainly due to excitonic recombination. The exact mechanism for emission in visible range is still not clear in spite of the various interpretations proposed by various groups [7–10]. Therefore, the understanding of the luminescence mechanism, as well as further improvement of the luminescence efficiency, is area of concern.The optical propertiesmainly depend on the size of the nanocrystals and nature of their capping. [11]. Some group also reported optimized ZnO@ZIF-8-based nanocomposite sensor shows markedly selective response to H2 [12]. Important factors for device fabrication are (i) the presence of unsaturated dangling bonds on the surface can generate, surface-passivated “dead layers”, (ii) the inability to withstand high processing temperatures and (iii) organic capping agents can decompose with high energy particle bombardment etc. A large number of synthesis routes [13, 14] are existing, Lu et al. reported 2D assembly of ZnO NCs on a substrate through a vapor phase transport technique [15]. G. Kenanakis reported Photoluminescence of ZnO nanostructures grown by the aqueous chemical growth technique [16]. High temperature XRD studies on ZnO nanopowder by ultrasonic mist chemical deposition were also reported [17]. To overcome the constraints involved in making nanophosphor based devices, we have synthesized a ZnO nanophosphor in a porous silica matrix using the sol-gel technique. The advantages associated with nanophosphor preparation is that there is no organic capping agent used to control the size, which suppresses the purity of the ZnO nanophosphor and the growth of the nanophosphor is limited to the size of the pore, which results in a confined particle size and other advantage of this method is that the silica network acts as a suitable binder that can be easily coated onto glass substrates either for characterization or for device fabrication. Various groups have been done on the UV photoluminescence (PL) in ZnO-based nanocomposites. Yao et al [18] reported band gap luminescence from ZnO in mesoporous silica, and they proposed that Zn–O–Si cross-linking bonds that formed at the interface between ZnO and the pore walls of silica had a great influence on the optical properties of ZnO/SiO2.The purpose of this study is to exploit the various possibilities of a nanophosphor-based device fabrication using a ZnO silica composite that combine the advantageous properties of the quantum size effect in semiconductor nanoparticles. We incorporated ZnO nanoparticles into a SiO2 matrix by the sol–gel method and found that the intensity of the UV PL band was greatly enhanced as compared to that of PVP capped ZnO. We suggest that the ZnO nanoparticles and SiO2 matrix, as well as the ZnO–SiO2 interface, are responsible for the UV PL enhancement effect. This device fabrication also provides appreciable encapsulation related thermal stability, and mechanical support to the nanoparticles.

2. Experiment

The nanosized ZnO:PVP sample was prepared by the sol–gel [19] method. Zinc acetate, Zn(CH3COO)2·2H2O and absolute ethanol were used in the synthesis without further purification. A 0.1 M ethanolic solution of zinc acetate was prepared by dissolving 0.015 mol of zinc acetate in 150 ml of ethanol. The flask was fitted with a condenser and refluxed while stirring for 3 h at 80°C. At the end of

this procedure, 150 ml of reaction product was obtained. Then Solution of PVP at 1.5 mM was also prepared in ethanol. About 15 ml of PVP solution in ethanol is added to the solution of Zinc acetate and mixed well. Then, 0.02 mol of lithium hydroxide powder ($LiOH \cdot H_2O$) was added to this precursor to give a final lithium concentration of 0.14 M. The mixture was then hydrolysed in an ultrasonic bath to accelerate the reaction. This hydrolysis reaction was continued at room temperature until lithium hydroxide powder was no longer visibly present. White precipitate (ZnO colloidal aggregation) was obtained by adding hexane into the solution. The supernatant was discarded, and the precipitate was re-dispersed in absolute ethanol and subjected recursively to this gentle precipitation procedure three times. The ZnO colloid prepared by these procedures was quite stable, and no precipitate was noticed even after three weeks of storage in a refrigerator. The powder sample for x-ray diffraction (XRD) measurements was prepared by drying the colloid at room temperature.

The $ZnO–SiO_2$ composite powder was prepared by the sol–gel method. Transparent silica alcogels were prepared by hydrolysis of an ethanol- (C_2H_5OH) diluted tetraethylorthosilicate [TEOS, $Si(OC_2H_5)_4$] in the presence of hydrochloric acid (HCl) as a catalyst to form monosilicic acid.

$$Si(C2H5)4 + 4H2O \xrightarrow{k} Si(OH)4 + 4C2H5OH \quad (1)$$

where, K is the catalyst (HCl).

The monosilicic acid is unstable and, hence, undergoes condensation to form silica alcogel.

$$nSi(OH)4 \rightarrow nSiO2 + 2nH2O, \quad (2)$$

From our previous experience, we decided to prepare an alcogel that has the optical transparency (~85% transmittance at an 800-nm wavelength) with a porosity and pore sizes of about 88% and 2–5 nm, respectively. This has been achieved using stoichiometric amounts of water required for the hydrolysis of TEOS and adjusting the pH of the solution to about 6. The details of the silica alcogel preparation can be obtained from other group publications [20–22].

First 5 ml of absolute alcohol, 5 ml of $Si(OEt)_4$, and some $Zn(CH_3COOH)_2$ were mixed together in a 25 ml conical flask to make a homogeneous solution (Zn/Si mole ratio 1:10). While stirring, 0.8 ml of 0.01M HCl aqueous solution was slowly dropped into the flask at room temperature. Then, 0.02 mol of lithium hydroxide powder ($LiOH \cdot H_2O$) was added to this precursor to give a final lithium concentration of 0.14 M. The solution was refluxed at 69°C for 2 h to form the sol. After the sol had been aged at room temperature for 24 h, 10 ml of absolute alcohol was added into the sol; this was followed by 10 min of stirring. The sol was dried at 60 °C in an oven to produce the $ZnO–SiO_2$ composite.

The nanoparticles synthesized thus were characterized in order to study structural and optical properties. XRD was performed on Rigaku D/max-2200 PC diffractometer operated at 40 kV/20 mA, using Cu Kα1 radiation with wavelength of 1.54Å in wide angle region from 10° to 80° on 2Θ scale. The size and morphology of prepared nanostructures were recorded on FEI transmission electron microscope model Technai 30 G2 S-Twin electron microscope operated at 300 KV accelerating voltage. PL studies were performed on a Perkin Elmer LS 55 luminescence spectrophotometerat room temperature.

3. Results and Discussion

The XRD spectra of the ZnO-PVP and $ZnO–SiO_2$ samples are shown in figure 1. The ZnO powder is crystalline and $ZnO-SiO_2$ is amorphous in nature and the grain size calculated from Scherrer equations is about 20-30 nm and 4-6 nm respectively. After encapsulation of ZnO with SiO_2 average sizes of the nanoparticles, as estimated from the Scherrer's formula, showed that higher temperature (5 h at 700 °C) does not influence the particle size very much as compared to the fresh sample annealed at 100 °C (as shown in figure 2), whereas there are sharp peaks in ZnO-PVP diffractogram as shown in Figure 3 which indicates increase in particle size, most probably as PVP is organic reagent unable to withstand that much high temperature. Silica, being a high-temperature melting material, might have effectively caged and encapsulated the individual ZnO nanoparticles, avoiding coalescence due to prolonged sintering effects. Whereas PVP is organic reagent which is unable in giving stable capping at higher temperature.

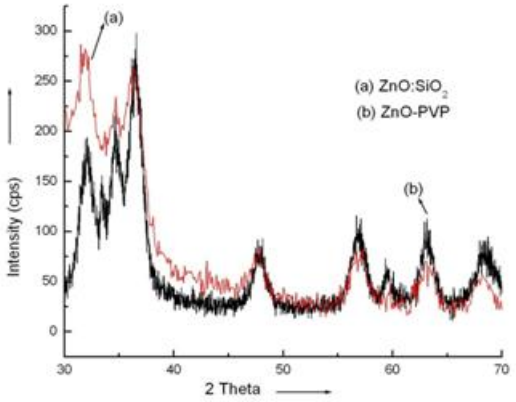

Figure 1: X-ray diffractogram of (a) $ZnO-SiO_2$ (b) ZnO-PVP

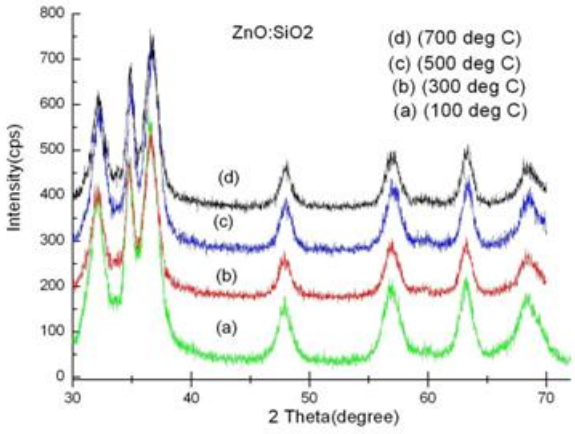

Figure 2: Temperature dependent X-ray diffractogram of $ZnO-SiO_2$

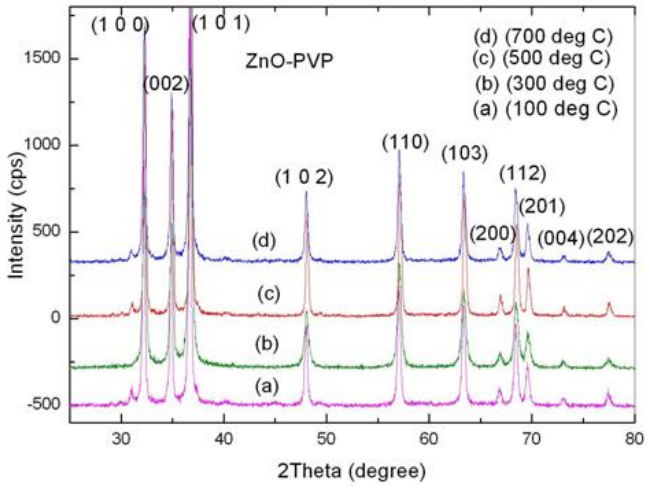

Figure 3: Temperature dependent X-ray diffractogram of ZnO-PVP

After establishing the crystal structure by XRD, it is very essential to examine the morphology and estimate the size, shape, and structure of the nanophosphors. With this view, the SEM and TEM observations were carried out. A typical TEM bright field image of the higher-ZnO content material showing the cluster was examined under the TEM operated at 200 kV (Figure 4 and 5). The ZnO–SiO_2 powder shows an amorphous nature where as ZnO-PVP shows crystalline nature and is confirmed by the SAED micrograph which is illustrated as the in Figure 6 and 7. It can be seen that the ZnO nanoparticles were homogeneously distributed in the SiO_2 matrix. The average size of the ZnO nanoparticles in the SiO_2 composite is about 3–6 nm as measured from the HRTEM micrograph shown in figure 4 where as ZnO-PVP nanoparticles size is about 20-30 nm as shown in figure 5. SEM micrograph of ZnO:SiO_2 nanoparticles shows spherical particles throughout the region with an average particle size of about 3–10 nm where as ZnO-PVP nanoparticles are irregular in shape as shown in figure 8 and 9. Furthermore, the average crystallite sizes of the nanophosphors calculated from the XRD and electron microscopy are nearly comparable to each other. The slight discrepancy of the values may be due to the very small sample area chosen for the TEM scan, and a statistical particle size distribution was taken into account.

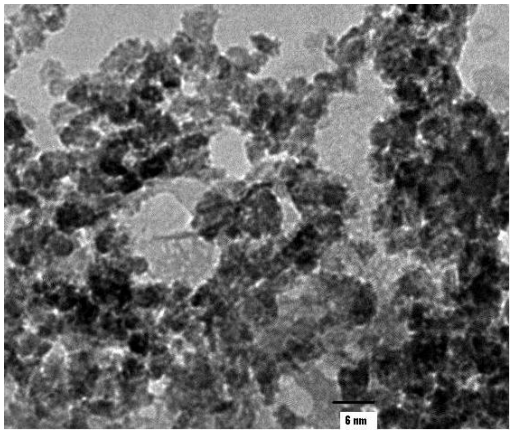

Figure 4: TEM micrograph of ZnO-SiO_2

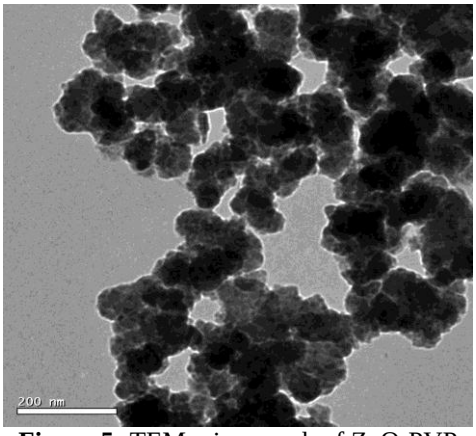

Figure 5: TEM micrograph of ZnO-PVP

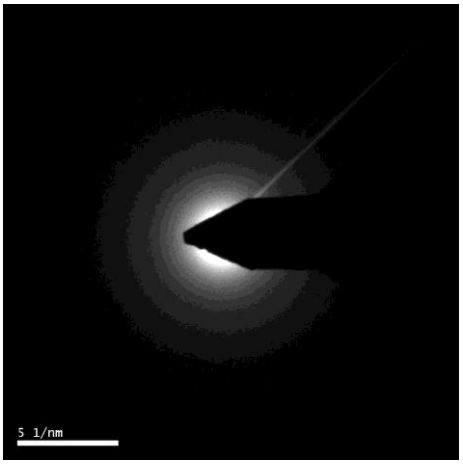

Figure 5: SAED pattern of ZnO-SiO_2

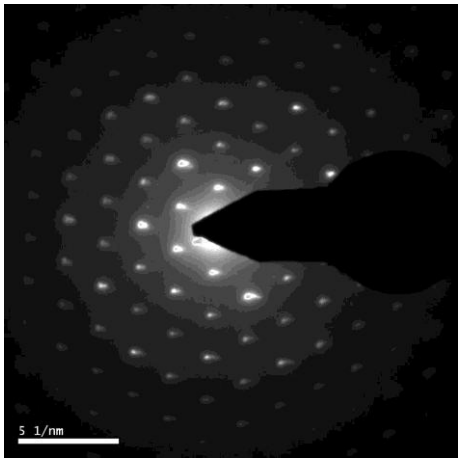

Figure 6: SAED pattern of ZnO-PVP

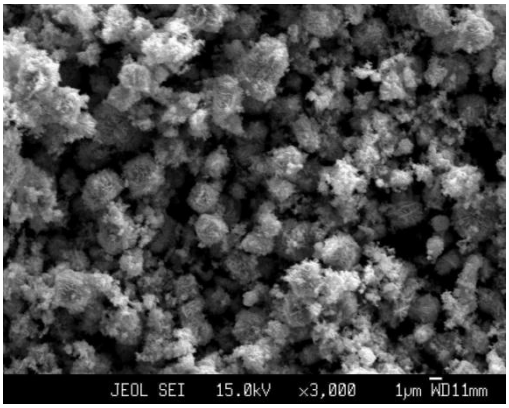

Figure 7: SEM micrograph of ZnO-SiO_2

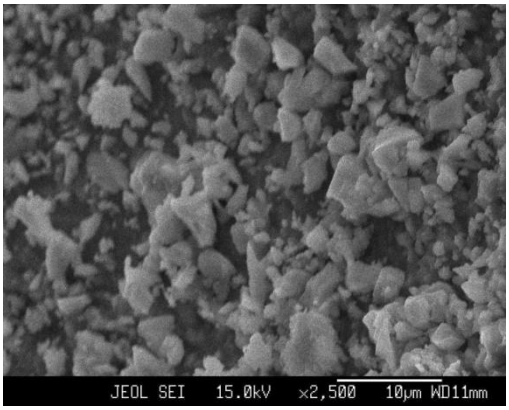

Figure 8: SEM micrograph of ZnO-PVP

4. PL Studies

In recent years, several researchers have shown interest in preparing ZnO in nanocrystalline texture inside a suitable matrix by using chemical routes with a view to understanding the effect of luminescence centres in newer environments [23, 24]. The PL spectra of the present work, recorded at room temperature (~300 K), showed three emission bands: (i) one UV excitonic and (ii) two visible defect level emissions. The visible emissions in ZnO may originate from various defect levels such as (a) structural impurities (doping) (b) intrinsic defects due to interstitial Zn ion (c) ionized oxygen vacancies etc. Several workers [25, 26, 27] have studied the effect of impurities by doping ZnO with different ions (Mn [26], Cu [25], In [27], etc). However, as no dopant was added in the present samples, structural impurities need not be considered as a factor influencing luminescence. As discussed in the following, an intrinsic defect due to oxygen vacancy seems applicable in explaining the prominent defect-related peaks in the PL spectra. This issue will be discussed in more detail below.

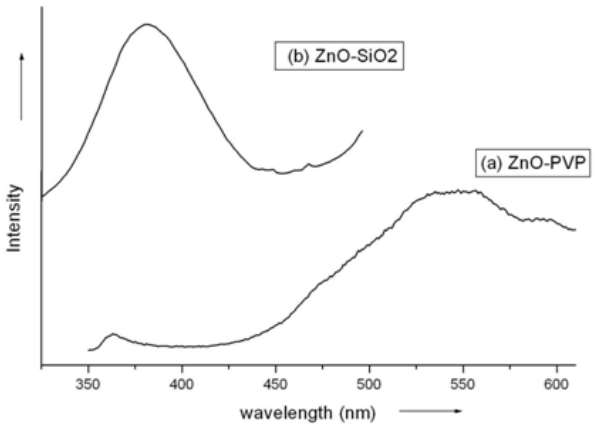

Figure 9: PL spectra of (a) ZnO-PVP excited with 277 nm light and (b) ZnO–SiO2 excited with 235 nm light.

Under excitation with 277 nm light, the PL spectra of the ZnO-PVP sample consist of a broad visible band centred at 552 nm and a very weak UV band centred at 365 nm (curve (a) in figure 9), which are for the defect state emission and the near-band-edge (NBE) emission respectively [28]. With a 235 nm exciting source light, an enhanced UV broad band was observed from the ZnO–SiO_2 composites (curve (b) in figure 9). In the PL spectra of the ZnO–SiO2 sample there are a main broad UV band centered at 380 nm with one inconspicuous shoulder centered at 470 nm. For comparison, we define the ratio R = IUV/IVIS as the ratio of the intensity of the UV emission to that of the visible emission at room temperature. The effect of the nanocomposite structure on the UV PL process is obvious: R for the ZnO–SiO2 sample is much greater than that for the ZnO –PVP sample. The relation of and/or differences between the UV PL processes for these two types of sample are more evident in the PLE spectra which were measured by monitoring the UV emission band. The results are illustrated in figure 10. The PLE spectra of the ZnO samples show a wide band at 260–340 nm, which is due to the process in which carriers are excited in ZnO nanoparticles [29]. On the other hand, the PLE spectra of the ZnO–SiO_2 samples contain not only a 260–340 nm band, but also a stronger band at 230 nm, which may originate from the SiO_2 matrix [30].

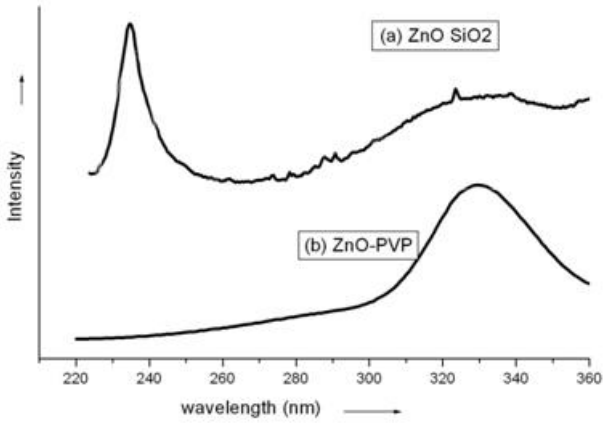

Figure 10: PLE spectra of (a) the 365 nm peak of ZnO-PVP and (b) the 380 nm peak of ZnO–SiO2.

This result implies that, in nanocomposites there are several mechanisms entangled in the UV emission, i.e. all of the ZnO nanoparticles, the ZnO–SiO_2 interface, and the SiO_2 matrix contributed to the UV emission. The interface between the ZnO particles and SiO_2 matrix may enhance the UV emission by two possible mechanisms. One possible mechanism is modifying the surface nature of the ZnO nanoparticles. Studies have shown that the luminescence efficiency of nanoparticles is strongly dependent on the nature of the surface, because small particles have a large surface-to-volume ratio. In the case of ZnO-PVP nanoparticles, surface states such as dangling bonds are usually involved in non-radiative processes, while O^{2-} ions provide a critical pathway for the visible emission band [31–32]. Embedding the ZnO nanoparticles in a SiO_2 matrix will reduce the density of surface dangling bonds and O^{2-} ions via Zn–O–Si, so reducing the probability of nonradiative and visible emission; in contrast, the UV emission probability will be increased. This passivation mechanism may contribute partly to the UV PL enhancement.

Another possible mechanism via which the interface may contribute for the UV PL enhancement is by creation of interface states where carriers can be trapped and recombine to emit UV light. As demonstrated previously, the net charge of the Zn atom in the Zn–O–Si bond is

positive. According to the general theory of defects, a positive centre in ZnO produces an attractive defect potential, attracting levels of the conduction band into the band gap and creating a donor state [33]. Due to the weak attractive potential, the Zn–O–Si interface state is shallow as compared with the ZnO:V_O and ZnO:Zn_I states. As a result, the energy level of the donor state created by Zn–O–Si may shift to 3.26 eV (380 nm) and act as a luminescence centre for the 380 nm band; i.e., carriers excited in ZnO and SiO2 may be trapped at the interface states and consequently recombine to emit a band at 380 nm. Because of the large interface-to-volume ratio in the nanocomposites, this process is greatly enhanced, resulting in enhancement of the UV emission efficiency.

In addition to the effect of the interface, the nanocomposite structure may contribute to the UV PL enhancement via enhancing the excitation process in the SiO_2 matrix and the luminescence process in the ZnO nanoparticles. In the nanocomposites, some of the carriers excited in the SiO_2 matrix may tunnel to the ZnO–SiO_2 interface or to ZnO nanoparticles and recombine, enhancing the UV band. On the other hand, SiO_2 provides a good coverage of the ZnO surface and may act as an energetic barrier preventing the escape of photogenerated carriers to outside the confined ZnO nanoparticles. However, more research is needed to elucidate the details.

On the basis of the above discussion, we illustrate the tentative excitation and emission processes of the 380 nm UV band in Figure 17 . First, a large number of carriers are excited in ZnO and SiO_2 via processes 1 and 2. Then some of the excited carriers are trapped at the interface and consequently recombine, emitting the band at 380 nm (process 3), while other excited carriers may recombine in the SiO_2 matrix and/or in ZnO nanoparticles, resulting in the 350 and 470 nm emission, as well as the band at 380 nm. All these processes may contribute to the enhancement of the UV PL in the nanocomposites.

5. Conclusions

The following conclusions can be drawn from the results of the studies on the effective capping of ZnO nanoparticles using Organic and Inorganic stabilizers. After encapsulation of ZnO with SiO_2 average sizes of the nanoparticles, as estimated from the Scherrer's formula, showed that higher temperature (5 h at 700 °C) does not influence the particle size very much as compared to the fresh sample annealed at 100 °C (as shown in figure 2), where as there are sharp peaks in ZnO-PVP diffractogram as shown in Figure 3 which indicates increase in particle size with temperature, most probably as PVP is organic reagent unable to withstand that much high temperature where as Silica, being a high-temperature melting material, might have effectively caged and encapsulated the individual ZnO nanoparticles, avoiding coalescence due to prolonged sintering effects.

SEM micrographs of ZnO:SiO_2 nanoparticles shows spherical particles where as irregular shape in ZnO-PVP. Furthermore, the average crystallite sizes of the nanophosphors calculated from the XRD and electron microscopy are nearly comparable to each other. The slight discrepancy of the values may be due to the very small sample area chosen for the TEM scan, and a statistical particle size distribution was taken into account.

The luminescence intensity of the UV emission in ZnO–SiO_2 nanocomposites prepared by the sol–gel method was much higher than that of sol–gel ZnO-PVP. New energy states are formed due to the presence of Zn–O–Si bonds at the interface. The PLE results show that both the ZnO nanoparticles and the SiO_2 matrix in the nanocomposites contribute to the luminescence process. Inorganic capping agent seemed to be the better capping agent as it can withstand high temperature, also having much higher luminescence intensity and shows monodispersed ZnO nanoparticles and can be utilized for device fabrication as all these properties are favorable for the same.

References

[1] Chen Y F, Tuan N T, Segawa Y, Ko H J, Hong S K and Yao T, Appl. Phys. Lett. 2001;78 :1469
[2] Zhang W H, Shi J L, Wang L Z and Yan D S, Chem. Mater. 2000; 12: 1408
[3] Shi G, Mo C M, Cai W L and Zhang L D, Solid State Commun. 2000; 115: 253
[4] Mo C M, Li Y H, Liu Y S, Zhang Y and Zhang L D, J. Appl. Phys. 1998; 83: 4389
[5] Li J F, Yao L Z, Ye C H, Mo C M, Cai W L, Zhang Y and Zhang L D, J. Cryst. Growth.2001; 223: 535
[6] Wang Y W, Zhang L D, Wang G Z, Peng X S, Chu Z Q and Liang C H, J. Cryst. Growth. 2002; 234: 171
[7] Guo L, Cheng J X, Li X Y, Yan Y J, Yang S H, Yang C L, Wang J N and Ge W K, Mater. Sci. Eng. C. 2001; 16:123
[8] Cannas C, Casu M, Lai A, Musinu A and Piccaluga G, J. Mater. Chem. 1999; 9: 1765
[9] Fujihara S, Naito H and Kimura T, Thin Solid Films.2001; 389: 227
[10] W. Vogel, P. H. Borse, N. Deshmukh, and S. K. Kulkarni, Langmuir.2000; 16: 2032.
[11] Tapas Kumar Kundu, Nantu Karak, Puspendu Barik, SatyajitSaha, Issue-NCRAMT. 2011; 1: 19
[12] Martin Drobek, Jae-Hun Kim, Mikhael Bechelany, Cyril Vallicari, Anne Julbe, and Sang Sub Kim, ACS Appl. Mater. Interfaces. 2016; 8: 8323.
[13] Chetan K. Kasar, Jaspal Bange. D.S.Patil, J Mater Sci: Mater Electron, DOI: 10.1007/s10854-017-6910-x :2017.
[14] A Wei1, X W Sun1, C X Xu, Z L Dong, Y Yang1, S T Tan1 and W Huang, Nanotechnology. 2006; 17: 6 .
[15] J. G. Lu, Z. Z. Ye, Y. Z. Zhang and Z. L. Wang, Appl. Phys. Lett. 2006; 23122: 89.
[16] G. Kenanakis, M. Androulidakic, E. Koudoumasa and N. Katsarakis, Superlattices and Microstructures. 2007;42: 473.
[17] Preetam Singh, Ashvani Kumar and Ashish Pandey, Bull. Mater. Sci. 2008;31 : 573.
[18] Sakohara S, Tickanen L D and Anderson M A, J. Phys. Chem. 1992; 96: 11086.
[19] A. Venkateswara Rao, N. N. Parvathy, and G. M. Pajonk, J. Mater. Sci. 1994; 29: 1807.

[20] P. B. Wagh, A. Venkateswara Rao, and D. Haranath, Mater. Chem. Phys. 1998; 53: 41.
[21] A. Venkateswara Rao, P. B. Wagh, D. Haranath, P. P. Risbud, and S. D.Kumbhare, Ceram. Int. 1999; 25: 505.
[22] Mo C M, Li Y H, Liu Y S, Zhang Y and Zhang L D, J. Appl. Phys. 1998; 83: 4389.
[23] Fujihara S, Naito H and Kimura T, Thin Solid Films. 2001; 389: 227
[24] Dingle R, Phys. Rev. Lett. 1969; 23:579.
[25] Liu M, Kitai A H and Mascher P, J. Lumin. 1992; 54: 35
[26] Ortiz A and Garcia M, Thin Solid Films. 1992; 207: 175
[27] Nyffenegger R M, Craft B, Shaaban M, Gorer S, Erley G and Penner R M, Chem. Mater. 1998; 10: 1120
[28] Guo Lin, Yang Shihe, Yang Chunlei, Yu Ping, Wang Jiannong, Ge Weikun and Wong G K L, Appl. Phys. Lett. 2000; 76: 2901
[29] Anedda A, Carbonaro C M, Corpino R and Raga F, Nucl. Instrum. Methods B. 1998; 141:719.
[30] Van Dijken A, Meulenkamp E A, Vanmaekelbergh D and Meijerink A, J. Lumin.2000; 454: 87.
[31] Van Dijken A, Makkinje J and MeijerinkA, J.Lumin. 2001;92 : 323.
[32] Van Dijken A, Meulenkamp E A, Vanmaekelbergh D and Meijerink A, J. Lumin. 2000; 90:123.
[33] Sun Y M, Xu P S, Shi C S, Xu F Q, Pan H B and Lu E D, J. Electron Spectrosc. 2001; 1123: 114